Flux-stabilized Majorana zero modes in coupled one-dimensional Fermi wires

Chun Chen, Wei Yan, C. S. Ting, Yan Chen, and F. J. Burnell

Phys. Rev. B **98**, 161106 — Published 8 October 2018

DOI: 10.1103/PhysRevB.98.161106

Flux-Stabilized Majorana Zero Modes in Coupled One-Dimensional Fermi Wires

Chun Chen,[1,*] Wei Yan,[2,3] C. S. Ting,[4] Yan Chen,[2,3] and F. J. Burnell[1]

[1]*School of Physics and Astronomy, University of Minnesota, Minneapolis, Minnesota 55455, USA*
[2]*Department of Physics and State Key Laboratory of Surface Physics, Fudan University, Shanghai 200433, China*
[3]*Collaborative Innovation Center of Advanced Microstructures, Nanjing 210093, China*
[4]*Texas Center for Superconductivity and Department of Physics, University of Houston, Houston, Texas 77204, USA*

(Dated: August 16, 2017)

One promising avenue to study one-dimensional (1D) topological phases is to realize them in synthetic materials such as cold atomic gases. Intriguingly, it is possible to realize Majorana boundary modes in a 1D number-conserving system consisting of two fermionic chains coupled only by pair-hopping processes [1]. It is commonly believed that significant interchain single-particle tunneling necessarily destroys these Majorana modes, as it spoils the $\mathbb{Z}_2$ fermion-parity symmetry that protects them. In this Letter, we present a new mechanism to overcome this obstacle, by piercing a (synthetic) magnetic π-flux through each plaquette of the Fermi ladder. Using bosonization, we show that in this case there exists an exact leg-interchange symmetry that is robust to interchain hopping, and acts as fermion parity at long wavelengths. We utilize density matrix renormalization group and exact diagonalization to verify that the resulting model exhibits Majorana boundary modes up to large single-particle tunnelings, comparable to the intrachain hopping strength. Our work highlights the unusual impacts of different topologically trivial band structures on these interaction-driven topological phases, and identifies a distinct route to stabilizing Majorana boundary modes in 1D fermionic ladders.

PACS numbers: 67.85.−d, 71.10.Pm, 03.67.Lx, 74.90.+n

The classification of topological phases in one dimension [2–4] revealed an intriguing array of possible new states of matter, with a variety of types of protected gapless boundary modes. Of these, one class that has generated considerable excitement recently is the one-dimensional (1D) topological superconductors first described by Ref. [5]. These have protected boundary Majorana zero modes, which harbor non-Abelian statistics [6–8] and hence are promising candidates for topological quantum computing [9, 10].

In practice, to obtain long-range superconducting (SC) order in 1D systems requires inducing superconductivity via coupling to a 3D bulk superconductor [11–21]; experimental progress in this direction has been made in several distinct solid-state systems [22–26]. Interestingly, however, it is also possible to host topological boundary modes in truly 1D platforms, in spite of the fact that these systems do not support long-range SC order, and are in fact gapless [1, 27–35]. This opens up the possibility of studying 1D fermionic topological phases in synthetic materials such as cold atomic gases [36–43], offering an attractive architecture with increased tunability.

One concrete model in this category was proposed by Ref. [1], who showed numerically that even starting from a lattice Hamiltonian with a topologically trivial band structure, a regime bearing the hallmarks of Majorana boundary modes can be accessed in an atomic two-leg ladder by introducing an interleg pair-hopping interaction. These boundary modes are protected by the conserved fermion parity of *one* of the wires, and are therefore robust provided that the single-particle interleg tunneling ($t_\perp$), which breaks this symmetry explicitly, is sufficiently small. A number of proposals [1, 32–34] for suppressing $t_\perp$ such that this regime may be experimentally realized ensued.

In this paper we propose a distinct route to overcome this obstacle: We begin with a different band structure, in which each plaquette of the ladder has a flux of π. We show that with pair hopping this model also has an interacting topological regime hosting Majorana boundary modes—which in this case are protected by a *unitary* symmetry preserved even in the presence of finite $t_\perp$. We bolster our theory with numerical evidence of Majorana boundary modes over a wide range of $t_\perp$. Our findings thus furnish an appealing mechanism to engineer topological boundary modes in a particle-conserving and strongly interacting system without the need to suppress $t_\perp$.

Fermionic flux ladder model.—Motivated by these considerations, we study an interacting two-leg ladder model of spinless fermions in a perpendicular magnetic field described by the following number-conserving Hamiltonian,

$$H = H_K + H_W, \tag{1}$$

$$H_K = -\sum_{n=0}^{L-2}[(t_\parallel e^{i\frac{\phi}{2}}c^\dagger_{n,0}c_{n+1,0}+t_\parallel e^{-i\frac{\phi}{2}}c^\dagger_{n,1}c_{n+1,1})+\text{H.c.}] - \sum_{n=0}^{L-1}(t_\perp c^\dagger_{n,0}c_{n,1}+\text{H.c.}), \tag{2}$$

$$H_W = +\sum_{n=0}^{L-2}(W c^\dagger_{n,0}c^\dagger_{n+1,0}c_{n,1}c_{n+1,1}+\text{H.c.}), \tag{3}$$

where $c^{(\dagger)}_{n,\ell}$ is the fermionic annihilation (creation) operator at rung n on the leg $\ell = 0, 1$. The intraleg and interleg single-particle tunneling strengths are $t_\parallel$ and $t_\perp$, respectively, and W (which we take to be negative throughout this work) is the pair-hopping strength. This band structure was studied by Ref. [44] in a two-leg ladder of spinful fermions. Two essential ingredients of the above model are the synthetic Peierls phase $\phi \in [0, \pi]$ per plaquette, and the interchain pair-hopping interaction H_W. Previous works have demonstrated the existence of Majorana boundary modes in this Hamiltonian at $\phi=0$ and $t_\perp=0$ based on a preserved fermion-number parity $\mathsf{P}_\ell := (-1)^{N_\ell}$, where N_ℓ is the particle-number operator of a single leg ℓ [1, 32–34]. Here we will show that when $\phi=\pi$, these boundary modes persist up to $t_\perp$ of order $t_\parallel$. Note that without pair hopping, the bare band H_K in (2) is topologically trivial, so that the model (1) requires interactions to realize the topological regime. This is necessarily the case for isolated 1D systems, where the total fermion number is conserved—in contrast to models based on e.g., Kitaev or spin-orbit-coupled (SOC) wires [45–47], where the Majorana modes may originate from nontrivial Bogoliubov–de Gennes band structures.

Indeed, the π-flux ladder model can be viewed as generalizing the SC proximitrized SOC nanowire model [15, 16] to a number-conserving setting. Specifically, the flux gives rise to the leg-momentum locking, similar to the spin-momentum locking in SOC systems. The interchain $t_\perp$ plays the role of a Zeeman field that opens gaps at band crossings. Finally, the quadratic p-wave pairing terms are replaced by the four-fermion pair-hopping terms to ensure number conservation. Notice that the flux-equals-π band structure corresponds to a spin-orbit interaction of infinite strength. This ensures that umklapp scattering is present at any filling in the π-flux model [44]—a significant advantage relative to an actual spin-orbit coupling, since in number-conserving systems these umklapp terms are essential to enabling the topological regime. Indeed as our 1D system is not exactly at half-filling, the particle-hole and chiral operations [48] are not symmetries of the wave-function, such that the topologically nontrivial state requires interactions.

Symmetry analysis.—Through our system contains decoupled gapless sector, its topological boundary modes might be understood using the symmetry classification of 1D *gapped* fermionic phases [3]. We therefore begin with a discussion of the underlying symmetries. Below we argue that the Majorana boundary modes are protected by a unitary $\mathbb{Z}_2$ leg-interchange symmetry $\mathsf{L_s}$ which takes $c_{n,0} \to (-1)^{n+1}c_{n,1}$, $c_{n,1} \to (-1)^{n+1}c_{n,0}$, where n indexes the site along the chain [49]. This is a symmetry only for $\phi=\pi$; we will see that its action is equivalent to that of an emergent fermion-parity operator via bosonization. Additionally, for any flux ϕ, there is an antiunitary time-reversal symmetry that combines complex conjugation with interchanging the two legs of the ladder, obeying $\mathsf{T}^2=+1$. Finally, there also exists an overall $U(1)$ fermion-number conservation. In our case its chief significance is that, unlike the situation considered by Ref. [3], only at exactly half-filling is a microscopic particle-hole symmetry possible. If $t_\perp=0$, the model has an additional exact $\mathbb{Z}_2$ symmetry, corresponding to the fermion parity of a single leg of the ladder, given by P_ℓ. It is this symmetry that protects the topological boundary modes observed by Ref. [1] at zero flux.

Bosonization and renormalization group analysis.—To understand the special role of the $\mathbb{Z}_2$ symmetry $\mathsf{L_s}$, we bosonize the model (1). For $\phi=\pi$, the kinetic Hamiltonian H_K has

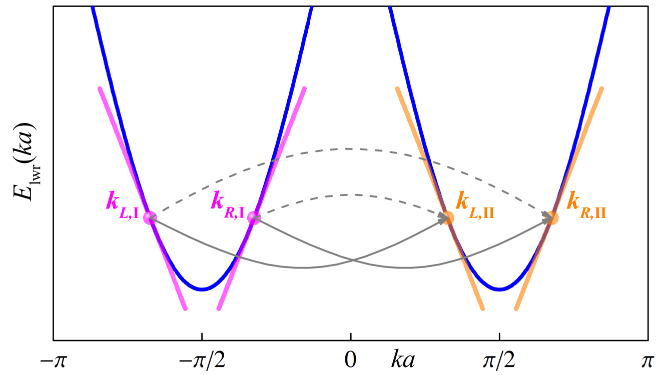

FIG. 1: Linearization of the lower band (blue solid line) at $\phi=\pi$. The obtained four chiral-fermion branches can be separated into valley-I (light magenta) and valley-II (light orange) that generalize the original chain degrees of freedom. Specifically, we depict the two types of umklapp processes that obey Eq. (4).

band energies $E_{\text{hgr/lwr}} = \pm\sqrt{t_\perp^2+4t_\parallel^2\sin^2(ka)}$, with band gap $2t_\perp$. Here we consider a system at less than half-filling, with the interaction scale W small relative to the bandwidth, such that we can project out the unoccupied band and focus only on the processes inside the lower band when treating H_W. Here the Fermi energy intersects the lower band at four separate Fermi points, as shown in Fig. 1.

Linearizing about these four Fermi points results in two right-moving (R) and two left-moving (L) fermion operators, which we distinguish using a valley index (I or II). Bosonizing these in the usual way, we have $\psi_{\kappa,\nu} \sim e^{i\varphi_{\kappa,\nu}}$, with $\kappa=R$ (L) and $\nu=\text{I}$ (II). We define the nonchiral bosonic fields: $\theta_c = \frac{1}{\sqrt{2}}(\theta_{\text{I}}+\theta_{\text{II}})$, $\theta_s = \frac{1}{\sqrt{2}}(\theta_{\text{I}}-\theta_{\text{II}})$, $\phi_c = \frac{1}{\sqrt{2}}(\phi_{\text{I}}+\phi_{\text{II}})$, $\phi_s = \frac{1}{\sqrt{2}}(\phi_{\text{I}}-\phi_{\text{II}})$, where $\theta_\nu = \frac{1}{\sqrt{2}}(\varphi_{R,\nu}-\varphi_{L,\nu})$, $\phi_\nu = \frac{1}{\sqrt{2}}(\varphi_{R,\nu}+\varphi_{L,\nu})$, such that $\varphi_{\kappa,\nu} = \frac{1}{2}[(\phi_c+\kappa\theta_c)+\nu(\phi_s+\kappa\theta_s)]$. After including appropriate Klein factors, the only nontrivial commutators among these nonchiral bosonic fields are $[\theta_c(x),\phi_c(x')] = -2i\pi\Theta(x'-x)$, $[\theta_s(x),\phi_s(x')] = 2i\pi\Theta(x-x')$, $[\theta_s(x),\phi_c(x')] = -2i\pi$, where $\Theta(x)$ is the Heaviside step function. The corresponding density and current operators are: $\rho_c = (1/\pi)\partial_x\theta_c$, $\rho_s = (1/\pi)\partial_x\theta_s$, $J_c = (1/\pi)\partial_x\phi_c$, $J_s = (1/\pi)\partial_x\phi_s$.

Bosonizing the interaction term H_W produces multiple four-fermion terms, of which only slowly-varying terms contribute in the continuum limit. When $\phi=\pi$, in addition to the usual momentum-conserving processes, this allows for intervalley umklapp scattering, since the Fermi points obey $k_{L,\text{I}} = -k_{R,\text{II}}$, $k_{R,\text{I}} = -k_{L,\text{II}}$, $k_{L,\text{II}}+k_{R,\text{II}} = \pi/a$, such that

$$k_{L,\text{II}} + k_{R,\text{II}} - k_{L,\text{I}} - k_{R,\text{I}} = \frac{2\pi}{a}. \qquad (4)$$

Eq. (4) is valid independent of the chemical potential within the lower band, but it will not hold if $\phi \neq \pi$ [44].

The resulting bosonized form of H decouples into a gapless charge sector and a gapped spin sector: $H \simeq H_c + H_s$, with

$$H_c = \int_x \frac{1}{2\pi}\{u_c K_c\left(\partial_x\phi_c(x)\right)^2 + \frac{u_c}{K_c}\left(\partial_x\theta_c(x)\right)^2\}, \tag{5}$$

$$\begin{aligned} H_s &= \int_x \frac{1}{2\pi}\{u_s K_s\left(\partial_x\phi_s(x)\right)^2 + \frac{u_s}{K_s}\left(\partial_x\theta_s(x)\right)^2\} \\ &+ \frac{2g_{um}}{(2\pi a)^2}\int_x \cos\left(2\phi_s(x)\right) - \frac{2g_{bs}}{(2\pi a)^2}\int_x \cos\left(2\theta_s(x)\right) \\ &- \frac{2g_{mx}}{(2\pi a)^2}\int_x \cos\left(2\theta_s(x)\right)\cdot\cos\left(2\phi_s(x)\right), \end{aligned} \tag{6}$$

where $\int_x \equiv \int dx$ and the associated coupling constants are given by $g_{um} = -\frac{aW}{\pi^2}\cos^2(k_{R,\mathrm{II}}a)(\sin^4\frac{\xi}{2} + \cos^4\frac{\xi}{2})$, $g_{bs} = -\frac{aW}{2\pi^2}\sin^2(k_{R,\mathrm{II}}a)\sin^2\xi$, and $g_{mx} = -\frac{aW}{2\pi^2}(\sin^4\frac{\xi}{2} + \cos^4\frac{\xi}{2})$. Here the wavefunction in the lower band at $k_{R,\mathrm{II}}$, has the form $(\cos\frac{\xi}{2},\ \sin\frac{\xi}{2})$ in the leg (i.e., $0,1$) basis [50]. Note that the g_{um}-term favors Cooper pairing while the competing g_{bs}-term favors a valley density-wave-type order. Moreover, owing to density-density interactions, the velocities and Luttinger parameters are renormalized. Particularly, for the spin channel: $u_s = \sqrt{(u+g)^2 - 4g^2\cos^2(2k_{R,\mathrm{II}}a)}$, $K_s = \sqrt{\frac{u+g+2g\cos(2k_{R,\mathrm{II}}a)}{u+g-2g\cos(2k_{R,\mathrm{II}}a)}}$, where $u = \frac{1}{2}v_F \equiv \frac{1}{2}\frac{dE_{\mathrm{lwr}}}{dk}\big|_{k=k_{R,\mathrm{II}}} > 0$ and $g = \frac{aW}{2(2\pi)^3}\sin^2\xi$.

As the charge sector is gapless, we will concentrate on the spin sector, which is responsible for the topological Majorana boundary modes. To determine which of the sine-Gordon terms in H_s dominates, we use the one-loop renormalization group (RG) flow equations: $dK_s(l)/dl = y_{um}^2(l)/2 - y_{bs}^2(l)K_s^2(l)/2$, $dy_{um}(l)/dl = (2-2K_s^{-1}(l))y_{um}(l)$, $dy_{bs}(l)/dl = (2-2K_s(l))y_{bs}(l)$, and $dy_{mx}(l)/dl = (2-2K_s(l)-2K_s^{-1}(l))y_{mx}(l)$, where $y_{um} = \frac{g_{um}}{2u\pi}$, $y_{bs} = \frac{g_{bs}}{2u\pi}$, and $y_{mx} = \frac{g_{mx}}{2u\pi}$ are dimensionless coupling constants. The g_{mx}-channel, involving both θ_s and ϕ_s, is power-counting irrelevant for any value of K_s and can be neglected. Accordingly, the gap-opening competition is between g_{um} and g_{bs}. If we take W to be negative, then for $3\pi/(4a) > k_{R,\mathrm{II}} > \pi/(2a)$ we have $K_s > 1$ and g_{um} is the only relevant coupling. In this regime the long-wavelength effective Hamiltonian is therefore expected to be $H_s \sim H_{\text{s-G}} = \int_{-\frac{L}{2}}^{\frac{L}{2}}\frac{dx}{2\pi}\{u_sK_s(\partial_x\phi_s(x))^2 + \frac{u_s}{K_s}(\partial_x\theta_s(x))^2 + \frac{g_{um}}{\pi a^2}\cos(2\phi_s(x))\}$. Note that for $W < 0$, $g_{um} > 0$ and the coefficient of the $\cos(2\phi_s)$ term is positive, contrary to the usual sine-Gordon model. As explained below, this sign flip, which arises from the particular umklapp processes that occur in the band structure for $\phi = \pi$, is crucial to ensuring that the staggered leg-interchange symmetry $\mathsf{L_s}$ acts like a fermion-parity operator. Indeed, for $W > 0$ and $3\pi/(4a) > k_{R,\mathrm{II}} > \pi/(2a)$ it is the negative coupling g_{bs} that is most relevant; this phase shows no numerical signatures of topological boundary modes, as discussed in [50].

We note that for flux $\phi \neq \pi$, the umklapp scattering leading to $H_{\text{s-G}}$ is no longer an effective zero (lattice)-momentum transfer process, and $\cos(2\phi_s(x))$ is replaced by $\cos(2\phi_s(x) - \delta\cdot x)$, where δ parameterizes the deviation of the flux from π. In this case we expect a commensurate-incommensurate transition which destroys the topological boundary modes at small *but finite* $\delta_c \sim \frac{1}{a}(y_{um})^{\frac{1}{2-2K_s^{-1}}}$ [51, 52]. This is consistent with numerical analysis [50], which suggests a transition for $|\phi - \pi| \gtrsim 0.05\pi$ into a phase in which θ_s is locked.

$\mathbb{Z}_2$ *symmetry and Majorana operators.*—Following Ref. [21] we can further derive the bosonized Majorana-boundary-mode operators by specifying the vacuum Hamiltonian density $\mathsf{H_{vac}}(x) = -\frac{2M_\infty}{\pi a}\sin(\theta_s(x))\cos(\theta_c(x))$, which amounts to sending the fermion mass outside the system to $+\infty$ on both legs of the ladder [53]. This fixes $\theta_s(x \in (-\infty, -\frac{L}{2})) = \pm\frac{\pi}{2} + 2\hat{n}^{(1)}_{\theta_s}\pi$ and $\theta_s(x \in (\frac{L}{2}, \infty)) = \pm\frac{\pi}{2} + 2\hat{n}^{(2)}_{\theta_s}\pi$. In the gapped bulk of the ladder, $\phi_s(x \in (-\frac{L}{2}, \frac{L}{2})) = -\frac{\pi}{2} + \hat{n}_{\phi_s}\pi$, where $\hat{n}^{(1,2)}_{\theta_s}$, $\hat{n}_{\phi_s}$ are integer operators. The two domain-wall Majorana operators are then: $\gamma_L \simeq e^{i\pi(\hat{n}^{(1)}_{\theta_s} + \hat{n}_{\phi_s})}$, $\gamma_R \simeq e^{i\pi(\hat{n}^{(2)}_{\theta_s} + \hat{n}_{\phi_s})}$. These satisfy the Majorana relations $\gamma^\dagger_{L/R} = \gamma_{L/R}$, $\gamma^2_{L/R} = 1$, $\{\gamma_L, \gamma_R\} = 0$, and define an emergent fermion parity $\mathsf{P_v} = i\gamma_L\gamma_R$. This acts on the spin fields within the gapped system via $\mathsf{P_v}\phi_s\mathsf{P_v}^{-1} = \phi_s - \pi$, $\mathsf{P_v}\theta_s\mathsf{P_v}^{-1} = \theta_s$. In particular, when g_{um} dominates the RG flow, $\mathsf{P_v}$ maps between the system's two classical ground states; when g_{bs} dominates the flow, it acts trivially on the two classical ground states.

Strictly speaking the operator $\mathsf{P_v}$ does not correspond to any microscopic symmetry for $|t_\perp| > 0$. (For $t_\perp = 0$, it can be interpreted as the fermion parity of one of the ladder's two legs.) However, at $\phi = \pi$ its action is equivalent to that of the microscopic $\mathbb{Z}_2$ symmetry $\mathsf{L_s}$, which acts on the bosonized field via $\mathsf{L_s}\phi_s(x)\mathsf{L_s}^{-1} = -\phi_s(x) \pmod{2\pi}$. Specifically, since g_{um} is positive, both $\mathsf{P_v}$ and $\mathsf{L_s}$ map between the two classical minima $|\pm\pi/2\rangle$ of the sine-Gordon potential, where $\phi_s(x)\,|\pm\pi/2\rangle = (\pm\pi/2 \bmod 2\pi)\,|\pm\pi/2\rangle$. Thus within the ground-state manifold, the action of $\mathsf{P_v}$ is equivalent to that of the exact symmetry of $\mathsf{L_s}$. Indeed, in a finite-size system, due to the proliferation of instanton processes [30, 54], the ground states of $H_{\text{s-G}}$ are split into $|\pm\rangle = \frac{1}{\sqrt{2}}(|\pi/2\rangle \pm |-\pi/2\rangle)$ whose energy difference is exponentially small in the system's size. The lowest two eigenstates therefore obey $\mathsf{P_v}\,|\pm\rangle = \pm\,|\pm\rangle$, $\mathsf{L_s}\,|\pm\rangle = \pm\,|\pm\rangle$, and can be labeled by their eigenvalues under the microscopic symmetry $\mathsf{L_s}$.

Comparing $\phi = \pi$ *with* $\phi = 0$.—As noted above, the topological state found in Ref. [1] at $\phi = 0$, $t_\perp = 0$ is protected by the symmetry P_ℓ corresponding to the conserved fermion parity of one of the ladder's legs. For $t_\perp = 0$, the operator $\mathsf{P_v}$ constructed from the Majorana boundary modes is exactly equal to P_ℓ, and therefore corresponds to an exact symmetry that protects the resulting topological boundary modes. In comparison, at $\phi = \pi$ we have found that $\mathsf{P_v}$'s action on the classical ground states is identical to that of the leg-exchange symmetry $\mathsf{L_s}$, which is not violated by finite $t_\perp$. Hence it is the particular action of $\mathsf{L_s}$ at this point which gives the topological boundary modes their enhanced stability. This result highlights the fact that different choices of topologically trivial band structures can have profound implications for interaction-driven topological phases.

In addition to these symmetry considerations, introducing $t_\perp$ at $\phi = 0$ has a significantly different impact on the band structure and umklapp processes than doing so at $\phi = \pi$, making the latter state more stable to this perturbation. For $\phi = t_\perp = 0$, the two chains' bands are identical. This overlap favors the momentum-conserving scattering processes that lead to the topological phase. However, increasing $t_\perp$ at $\phi = 0$ separates the two bands and creates a Fermi-velocity mismatch, which disfavors these processes, ultimately causing the spin gap to close at a small but finite value of $t_\perp$ [1]. By contrast, when $\phi = \pi$, the two valleys where the chains' bands cross the Fermi surface are maximally separated by a wave vector π/a, and remain symmetric with a finite $t_\perp$. In this case the Fermi-velocity mismatch is absent, and the spin gap persists up to large values of $t_\perp$. Thus the different nontopological band structures play a key role in making the topological Majorana modes robust (fragile) against $t_\perp$ at $\phi = \pi$ ($\phi = 0$), consistent with the fact that $t_\perp$ breaks P_ℓ but preserves L_s.

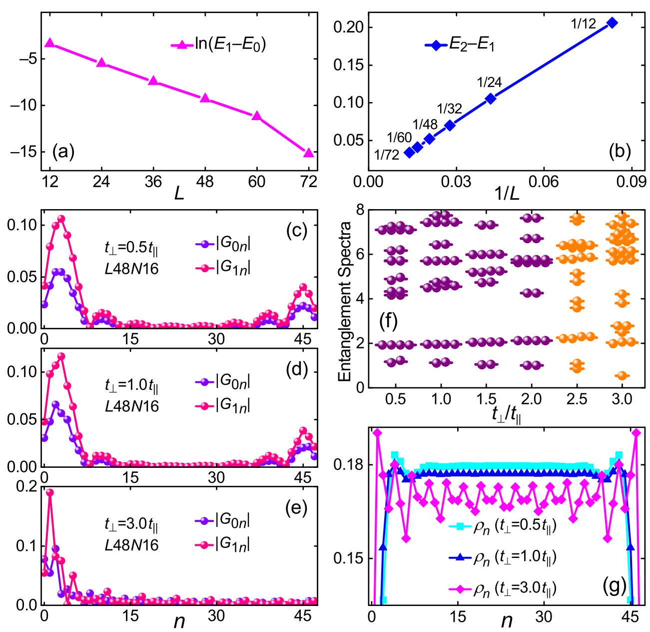

FIG. 2: Numerical signatures of the topological phase. (a) and (b): Scaling of energy gaps as functions of L from DMRG. (a) shows that the energy difference between the first two lowest-lying eigenstates of (1) decays exponentially with L. The protected ground-state manifold is separated from the rest of the spectrum by a gap that decreases inversely with L, as shown in (b). Here $W = -1.7t_\parallel$, $t_\perp = 0.5t_\parallel$, $\phi = \pi$, $N/L = 1/3$. (c)–(g): Transition out of the topological phase at large $t_\perp$ for fixed $W = -1.7t_\parallel$, $\phi = \pi$, $L = 48$, $N = 16$. (c)–(e) demonstrate the edge mode via the nonlocal correlations [1, 33, 34] in single-particle Green functions. At $t_\perp = 3.0t_\parallel$, the edge mode disappears indicating the transition to a trivial state. This is in accordance with (f) and (g) which show the corresponding evolutions of entanglement spectra and local fermion densities as the transition is approached.

Numerical verification.—Simulations based on density matrix renormalization group (DMRG) [55] and exact diagonalization (ED) [56] have been performed to solve the lattice model (1) at $\phi = \pi$ and $t_\perp = 0.5t_\parallel$. The numerical outcomes provide strong evidence supporting our theoretical predictions. Fig. 2(a) demonstrates that in the low-population region ($N/L = 1/3$), when pair hopping is strong ($W = -1.7t_\parallel$), the energy gap between the ground state and the 1st excited state closes exponentially as the ladder's size L increases. As anticipated, these two nearly degenerate eigenstates are distinguished by their eigenvalues of L_s: The ground (1st excited) state has eigenvalue $+1$ (-1). In contrast, the resulting ground-state manifold is further separated from the rest of the spectrum by a gap which only decreases inversely with L (Fig. 2(b)). This power-law gap closing is resulting from the decoupled gapless charge sector. Moreover, the topological Majorana boundary modes can be characterized via the nonlocal correlations [1, 33, 34] in the single-particle Green functions $G_{mn} \coloneqq \langle c^\dagger_{m,0} c_{n,0}\rangle = \langle c^\dagger_{m,1} c_{n,1}\rangle$. These are apparent for a range of $t_\perp$ values in the topological regime (Figs. 2(c)–(d)). The presence of the edge states also gives rise to a twofold degeneracy in the entanglement spectrum (ES) [2, 57] on the central bond (Fig. 2(f)). These DMRG results have been confirmed by ED for small system sizes.

As discussed in [50], adding a small L_s-symmetry-breaking perturbation to (1) causes the ES degeneracy to lift, and the energy gap $E_1 - E_0$ to deviate from the exponentially small splitting observed in Fig. 2(a). Further, the topological properties appear stable to adding a Rashba-like term, which preserves L_s but breaks the antiunitary symmetry T. This supports our claim that the topological boundary modes are protected by the unitary L_s symmetry at $\phi = \pi$ and $t_\perp \neq 0$.

For sufficiently large $t_\perp$, a phase transition out of the topological regime is observed. Fig. 2(e) shows a value $t_\perp > t_{\perp,\mathrm{c}} \approx 2.5t_\parallel$, for which the nonlocal correlations in G_{mn} are absent. Further, as shown by Fig. 2(f), the ES degeneracy apparent for $t_\perp < t_{\perp,\mathrm{c}}$ is lifted and the lowest level is clearly nondegenerate at $t_\perp = 3.0t_\parallel$. Our numerics suggest that the transition is toward a state with density-wave order at large $t_\perp$: For $t_\perp > t_{\perp,\mathrm{c}}$, the fermion-density profile $\rho_n \coloneqq \langle c^\dagger_{n,0} c_{n,0}\rangle = \langle c^\dagger_{n,1} c_{n,1}\rangle$ in Fig. 2(g) evolves from a uniform distribution toward an oscillatory pattern. Additionally, for $t_\perp \geq 3.0t_\parallel$, the two lowest-energy eigenstates split and both have L_s eigenvalues of $+1$ [50]. All the above observations suggest that once $t_\perp > t_{\perp,\mathrm{c}}$, the Majorana boundary modes disappear.

Experimental feasibility.—In cold-atom laboratories, strong synthetic magnetic fields can be simulated in optical lattices by synthetic-dimensions and optical-atomic-clocks techniques [58–67]. This makes it possible to generate a significant flux per plaquette. For example, in quasi-1D fermionic ladders and Hall ribbons, the flux ϕ can reach 1.31π per plaquette, and chiral edge states have been detected [63–66]. Ref. [1] also describes an atomic scheme for creating the pair-hopping interaction. These developments make the prospect of realizing flux-stabilized Majorana zero modes a possibility in the near future.

To summarize, we have shown that by threading π-flux through each plaquette, interaction-driven Majorana bound states in fermionic ladders may be stabilized in the presence of single-particle interleg tunneling. *En route* we have established a connection between a microscopic $\mathbb{Z}_2$ leg-exchange symmetry present only at this flux value and the action of an emergent fermion-parity operator in the long-wavelength bosonized theory. We have also highlighted the advantages of the π-flux state in fostering umklapp processes which generate the spin gap enabling this topological regime. Our theory has been substantiated by extensive DMRG and ED calculations.

C. C. thanks M. D. Schulz for discussions. Part of the simulation is developed from ALPS package [68]. C. C. and F. J. B. are supported by NSF-DMR 1352271 and by the Sloan Foundation FG-2015-65927. W. Y. and Y. C. are supported by the National Natural Science Foundation of China (Grant Nos. 11625416, 11474064, and 11274069). C. S. T. is supported by the Robert A. Welch Foundation under Grant No. E-1146.

C. C. and W. Y. contributed equally to this work.

* Corresponding author.
cchen@physics.umn.edu

[1] C. V. Kraus, M. Dalmonte, M. A. Baranov, A. M. Läuchli, and P. Zoller, Phys. Rev. Lett. **111**, 173004 (2013).
[2] F. Pollmann, A. M. Turner, E. Berg, and M. Oshikawa, Phys. Rev. B **81**, 064439 (2010).
[3] L. Fidkowski and A. Kitaev, Phys. Rev. B **83**, 075103 (2011).
[4] X. Chen, Z.-C. Gu, and X.-G. Wen, Phys. Rev. B **83**, 035107 (2011).
[5] A. Y. Kitaev, Phys.-Usp. **44**, 131 (2001).
[6] J. Alicea, Y. Oreg, G. Refael, F. von Oppen, and M. P. A. Fisher, Nat. Phys. **7**, 412 (2011).
[7] J. D. Sau, S. Tewari, and S. Das Sarma, Phys. Rev. B **82**, 052322 (2010).
[8] F. Hassler, A. R. Akhmerov, C.-Y. Hou, and C. W. J. Beenakker, New J. Phys. **12**, 125002 (2010).
[9] C. Nayak, S. H. Simon, A. Stern, M. Freedman, and S. Das Sarma, Rev. Mod. Phys. **80**, 1083 (2008).
[10] S. Das Sarma, M. Freedman, and C. Nayak, npj Quantum Information **1**, 15001 (2015).
[11] L. Fu and C. L. Kane, Phys. Rev. Lett. **100**, 096407 (2008).
[12] L. Fu and C. L. Kane, Phys. Rev. B **79**, 161408 (2009).
[13] J. Alicea, Phys. Rev. B **81**, 125318 (2009).
[14] J. D. Sau, R. M. Lutchyn, S. Tewari, and S. Das Sarma, Phys. Rev. Lett. **104**, 040502 (2010).
[15] R. M. Lutchyn, J. D. Sau, and S. Das Sarma, Phys. Rev. Lett. **105**, 077001 (2010).
[16] Y. Oreg, G. Refael, and F. von Oppen, Phys. Rev. Lett. **105**, 177002 (2010).
[17] J. Alicea, Rep. Prog. Phys. **75**, 076501 (2012).
[18] M. M. Vazifeh and M. Franz, Phys. Rev. Lett. **111**, 206802 (2013).
[19] J. Klinovaja, P. Stano, A. Yazdani, and D. Loss, Phys. Rev. Lett. **111**, 186805 (2013).
[20] B. Braunecker and P. Simon, Phys. Rev. Lett. **111**, 147202 (2013).
[21] D. J. Clarke, J. Alicea, and K. Shtengel, Nat. Commun. **4**, 1348 (2013).
[22] V. Mourik, K. Zuo, S. M. Frolov, S. R. Plissard, E. P. A. M. Bakkers, and L. P. Kouwenhoven, Science **336**, 1003 (2012).
[23] A. Das, Y. Ronen, Y. Most, Y. Oreg, M. Heiblum, and H. Shtrikman, Nat. Phys. **8**, 887 (2012).
[24] M. T. Deng, C. L. Yu, G. Y. Huang, M. Larsson, P. Caroff, and H. Q. Xu, Nano Lett. **12**, 6414 (2012).
[25] S. Nadj-Perge, I. K. Drozdov, J. Li, H. Chen, S. Jeon, J. Seo, A. H. MacDonald, B. A. Bernevig, and A. Yazdani, Science **346**, 602 (2014).
[26] S. M. Albrecht, A. P. Higginbotham, M. Madsen, F. Kuemmeth, T. S. Jespersen, J. Nygård, P. Krogstrup, and C. M. Marcus, Nature **531**, 206 (2016).
[27] G. Ortiz, J. Dukelsky, E. Cobanera, C. Esebbag, and C. Beenakker, Phys. Rev. Lett. **113**, 267002 (2014).
[28] G. Ortiz and E. Cobanera, Ann. Phys. **372**, 357 (2016).
[29] G. Y. Cho, R. Soto-Garrido, and E. Fradkin, Phys. Rev. Lett. **113**, 256405 (2014).
[30] L. Fidkowski, R. M. Lutchyn, C. Nayak, and M. P. A. Fisher, Phys. Rev. B **84**, 195436 (2011).
[31] J. D. Sau, B. I. Halperin, K. Flensberg, and S. Das Sarma, Phys. Rev. B **84**, 144509 (2011).
[32] M. Cheng and H.-H. Tu, Phys. Rev. B **84**, 094503 (2011).
[33] N. Lang and H. P. Büchler, Phys. Rev. B **92**, 041118 (2015).
[34] F. Iemini, L. Mazza, D. Rossini, R. Fazio, and S. Diehl, Phys. Rev. Lett. **115**, 156402 (2015).
[35] J. Ruhman, E. Berg, and E. Altman, Phys. Rev. Lett. **114**, 100401 (2015).
[36] C. Zhang, S. Tewari, R. M. Lutchyn, and S. Das Sarma, Phys. Rev. Lett. **101**, 160401 (2008).
[37] M. Sato, Y. Takahashi, and S. Fujimoto, Phys. Rev. Lett. **103**, 020401 (2009).
[38] C. Chen, Phys. Rev. Lett. **111**, 235302 (2013).
[39] C. Qu, Z. Zheng, M. Gong, Y. Xu, L. Mao, X. Zou, G. Guo, and C. Zhang, Nat. Commun. **4**, 2710 (2013).
[40] W. Zhang and W. Yi, Nat. Commun. **4**, 2711 (2013).
[41] X.-J. Liu and H. Hu, Phys. Rev. A **88**, 023622 (2013).
[42] I. Bloch, J. Dalibard, and W. Zwerger, Rev. Mod. Phys. **80**, 885 (2008).
[43] N. Goldman, J. C. Budich, and P. Zoller, Nat. Phys. **12**, 639 (2016).
[44] A. Jaefari and E. Fradkin, Phys. Rev. B **85**, 035104 (2012).
[45] L. Fidkowski and A. Kitaev, Phys. Rev. B **81**, 134509 (2010).
[46] E. M. Stoudenmire, J. Alicea, O. A. Starykh, and M. P. A. Fisher, Phys. Rev. B **84**, 014503 (2011).
[47] Y.-H. Chan, C.-K. Chiu, and K. Sun, Phys. Rev. B **92**, 104514 (2015).
[48] A. P. Schnyder, S. Ryu, A. Furusaki, and A. W. W. Ludwig, Phys. Rev. B **78**, 195125 (2008).
[49] This symmetry was also noted by Ref. [44].
[50] See Supplemental Material for relevant discussions.
[51] H. J. Schulz, Phys. Rev. B **22**, 5274 (1980).
[52] T. Giamarchi, *Quantum Physics in One Dimension*, (Oxford University Press, New York, 2004).
[53] A. Keselman and E. Berg, Phys. Rev. B **91**, 235309 (2015).
[54] C. Chen and F. J. Burnell, Phys. Rev. Lett. **116**, 106405 (2016).
[55] S. R. White, Phys. Rev. Lett. **69**, 2863 (1992).
[56] A. W. Sandvik, AIP Conf. Proc. **1297**, 135 (2010).
[57] H. Li and F. D. M. Haldane, Phys. Rev. Lett. **101**, 010504 (2008).
[58] M. Aidelsburger, M. Atala, S. Nascimbène, S. Trotzky, Y.-A. Chen, and I. Bloch, Phys. Rev. Lett. **107**, 255301 (2011).
[59] M. Aidelsburger, M. Atala, M. Lohse, J. T. Barreiro, B. Paredes,

and I. Bloch, Phys. Rev. Lett. **111**, 185301 (2013).

[60] H. Miyake, G. A. Siviloglou, C. J. Kennedy, W. C. Burton, and W. Ketterle, Phys. Rev. Lett. **111**, 185302 (2013).

[61] M. Atala, M. Aidelsburger, M. Lohse, J. T. Barreiro, B. Paredes, and I. Bloch, Nat. Phys. **10**, 588 (2014).

[62] C. J. Kennedy, W. C. Burton, W. C. Chung, and W. Ketterle, Nat. Phys. **11**, 859 (2015).

[63] L. F. Livi, G. Cappellini, M. Diem, L. Franchi, C. Clivati, M. Frittelli, F. Levi, D. Calonico, J. Catani, M. Inguscio, and L. Fallani, Phys. Rev. Lett. **117**, 220401 (2016).

[64] F. A. An, E. J. Meier, and B. Gadway, Sci. Adv. **3**, e1602685 (2017).

[65] S. Kolkowitz, S. L. Bromley, T. Bothwell, M. L. Wall, G. E. Marti, A. P. Koller, X. Zhang, A. M. Rey, and J. Ye, Nature **542**, 66 (2017).

[66] M. Mancini, G. Pagano, G. Cappellini, L. Livi, M. Rider, J. Catani, C. Sias, P. Zoller, M. Inguscio, M. Dalmonte, and L. Fallani, Science **349**, 1510 (2015).

[67] J. Struck, C. Ölschläger, M. Weinberg, P. Hauke, J. Simonet, A. Eckardt, M. Lewenstein, K. Sengstock, and P. Windpassinger, Phys. Rev. Lett. **108**, 225304 (2012).

[68] M. Dolfi, B. Bauer, S. Keller, A. Kosenkov, T. Ewart, A. Kantian, T. Giamarchi, and M. Troyer, Comput. Phys. Commun. **185**, 3430 (2014).